

1 **Lymph/angiogenesis contribute to sex differences in lung cancer through ERalpha**
2 **signalling**

3

4 Charline Dubois¹, Natacha Rocks¹, Silvia Blacher¹, Irina Primac¹, Anne Gallez¹, Melissa
5 García-Caballero¹, Céline Gérard¹, Laurent Brouchet², Agnès Noël¹, Françoise Lenfant³,
6 Didier Cataldo¹, Christel Pequeux¹

7

8 ¹ Laboratory of Tumour and Development Biology, GIGA-Cancer, University of Liège, CHU-
9 B23, B-4000 Liège, Belgium

10 ² Thoracic surgery department, University Hospital CHU Toulouse, F-31432 Toulouse,
11 France

12 ³ INSERM UMR1048, Institut des maladies métaboliques et cardiovasculaires – I2MC,
13 University of Toulouse III Paul Sabatier, UPS, F-31432 Toulouse, France

14

15 **Correspondence** should be addressed to C. Pequeux, University of Liège, Laboratory of
16 Tumour and Development Biology, GIGA-Cancer, Institute of Pathology B23, 13 Hippocrate
17 avenue, B-4000 Liège, Belgium. E-mail: C.Pequeux@uliege.be, Tel. +32 4 366 2217, +32 4
18 366 2569, Fax. +32 4 366 2936.

19

20 **Short title:** Sex differences in lung cancer

21

22 **Keywords:** lymphangiogenesis, angiogenesis, lung cancer, estrogen receptor, sex, gender,
23 tamoxifen, microenvironment

24

25 **Word count:** 4,962 words

26 **Abbreviations:**

- 27 **bFGF** basic Fibroblast Growth Factor
- 28 **CD31** Cluster of Differentiation 31
- 29 **COPD** Chronic Obstructive Pulmonary Disease
- 30 **Cx** Castrated
- 31 **DAPI** 4',6-diamidino-2-phénylindole
- 32 **DMEM** Dulbecco's Modified Eagle Medium
- 33 **DMSO** dimethylsulfoxyde
- 34 **E2** 17b-oestradiol
- 35 **EdU** 5-ethynyl-2'-deoxyuridine
- 36 **EGF** Epidermal Growth Factor
- 37 **EGFR** Epidermal Growth Factor Receptor
- 38 **ER** Estrogen Receptor
- 39 **FBS** Foetal Bovine Serum
- 40 **FBS cs** dextran-coated charcoal treated Foetal Bovine Serum
- 41 **GPCR** G Protein-coupled Estrogen Receptor 1
- 42 **HRT** Hormone Replacement Therapy
- 43 **LLC** Lewis Lung Carcinoma
- 44 **Luc** Luciferase-transfected
- 45 **LYVE1** Lymphatic vessel endothelial hyaluronan receptor 1
- 46 **OVX** Ovariectomised
- 47 **PDPN** Podoplanin
- 48 **Tmx** Tamoxifen
- 49 **VEGF** Vascular Endothelial Growth Factor
- 50 **VEGFR2** Vascular Endothelial Growth Factor Receptor 2

51 Abstract

52 Estrogen signalling pathways are emerging targets for lung cancer therapy. Unravelling the
53 contribution of estrogens in lung cancer development is a pre-requisite to support the
54 development of sex-based treatments and to identify patients who could potentially benefit
55 from anti-estrogen treatments. In this study, we highlight the contribution of lymphatic and
56 blood endothelia in the sex-dependent modulation of lung cancer. The orthotopic graft of
57 syngeneic lung cancer cells into immunocompetent mice showed that lung tumours grew
58 faster in female mice than in males. Moreover, estradiol (E2) promoted tumour development
59 in female mice and increased lymph/angiogenesis and levels of VEGFA and bFGF in lung
60 tumours of females through an estrogen receptor (ER) alpha-dependent pathway.
61 Furthermore, while treatment with ERbeta antagonist was inefficient, ERalpha antagonist
62 (MPP) and tamoxifen decreased lung tumour volumes, altered blood and lymphatic
63 vasculature and reduced VEGFA and bFGF levels in females, but not in males. Finally, the
64 quantification of lymphatic and blood vasculature of lung adenocarcinoma biopsies from
65 patients aged between 35 to 55 years old revealed more extensive lymphangiogenesis and
66 angiogenesis in tumour samples issued from women than from men. In conclusion, our
67 findings highlight an E2/ERalpha-dependent modulation of lymphatic and blood vascular
68 components of lung tumour microenvironment. Our study has potential clinical implication in
69 a personalised medicine perspective by pointing to the importance of estrogen status or
70 supplementation on lung cancer development that should be considered to adapt therapeutic
71 strategies.

72

73 **Introduction**

74 Development of personalised medicine in cancer care is the challenge of the 21st
75 century (Schleiden, et al. 2013). To ensure that patients benefit from the most appropriate
76 therapies, it is mandatory to identify specific mechanisms underlying individual responses to
77 therapies. There is now increasing clinical evidence linking sex differences to lung diseases
78 such as asthma, chronic obstructive pulmonary disease (COPD), as well as lung cancer
79 (Townsend, et al. 2012).

80 Historically, incidence rates of lung cancer were higher among men than women. This
81 pattern has now reversed in young population, since lung cancer incidence rates of lung
82 cancer are currently higher among young women than men (Jemal, et al. 2018; Lewis, et al.
83 2014). These observations cannot be fully explained by sex differences in smoking
84 behaviours. Population-based studies and clinical trials have also identified disparities in age,
85 smoking practices and histological subtypes between men and women (Katcoff, et al. 2014;
86 Wakelee, et al. 2006). Among non-smokers, women are 2.5-fold more susceptible than men to
87 develop lung cancer at a younger age and they display a higher prevalence for
88 adenocarcinoma (Siegfried 2001; Townsend et al. 2012; Wakelee, et al. 2007). Two major
89 pathways could contribute to these differences: the epidermal growth factor (EGF)/EGFR and
90 sex steroids (Cadranel, et al. 2011; Siegfried and Stabile 2014).

91 Clinical and experimental data strongly support a contribution of estrogens to lung
92 cancer development (Rodriguez-Lara, et al. 2018; Siegfried and Stabile 2014). Indeed,
93 elevated 17 β -oestradiol (E2) levels and higher expression of aromatase predict lower overall
94 survival in lung cancer patients (Mah, et al. 2007). Moreover, observational series show that
95 breast cancer patients receiving anti-estrogen therapy exhibit a reduced risk of developing
96 subsequent lung cancer and display lower mortality rates from lung cancer (Bouchardy, et al.

97 2011; Chu, et al. 2017). Exogenous E2 administration was linked to an increased lung tumour
98 growth of human tumour xenografts in female immunodeficient mice (Stabile, et al. 2002), as
99 well as boosted lung tumour development in a transgenic animal model (Hammoud, et al.
100 2008). However, the potential influence of menopausal hormone therapy (MHT) on lung
101 cancer incidence and survival remains unclear (Chlebowski, et al. 2016; Greiser, et al. 2010;
102 Schabath, et al. 2004). Overall, the contribution of estrogens in lung cancer is largely studied
103 and debated, especially regarding the complexity of the mechanisms sustaining their action.
104 Therefore, the use of patient-adapted anti-estrogen therapy still remains poorly considered for
105 lung cancer.

106 Tumour microenvironment, especially lymphatic and blood vasculatures, strongly
107 contributes to tumour development and dissemination (De Palma, et al. 2017; Dieterich and
108 Detmar 2016; Paupert, et al. 2011). Although E2 has been shown to regulate angiogenesis,
109 there is still a paucity of data regarding its effect on lymphatic endothelium, especially during
110 tumour lymphangiogenesis. Nevertheless, lymphedema, a lymphatic disorder associated to
111 accumulation of fat and fibrosis in limbs due to impaired lymphatic function, is related to
112 hormonal status and is sex linked (Alitalo, et al. 2005). Recent reviews highlighted the organ-
113 specificity of both lymphatic (Petrova and Koh 2018; Wong, et al. 2018) and vascular beds
114 (Nowak-Sliwinska, et al. 2018). Despite an abundant literature showing a direct pro-tumour
115 impact of E2 on lung cancer cells expressing estrogen receptors (ERs), little is known about
116 its effects on lung tumour microenvironment, especially lymphangiogenesis or angiogenesis
117 associated to lung cancer.

118 E2 binds two major receptors, ER alpha (ERa) and ER beta (ERb), belonging to the
119 nuclear receptor family (Hamilton, et al. 2017) and the G coupled-protein estrogen receptor
120 (GPER) (Barton, et al. 2017), a seven transmembrane-domain protein. Several studies
121 evidenced that human lung cancer cells predominantly express ERb (reviewed in (Baik and

122 Eaton 2012; Rodriguez-Lara et al. 2018) and that ER β sustains lung tumour growth in murine
123 models (Hershberger, et al. 2009; Pietras, et al. 2005; Tang, et al. 2014; Zhao, et al. 2011).
124 Otherwise, ER α -dependent growth-promoting genes are up-regulated in lung cancer (Pietras
125 et al. 2005; Pietras and Marquez-Garban 2007) and ER α expression is increased in lung
126 tumours from women (Raso, et al. 2009; Rouquette, et al. 2012). In addition, GPER is also
127 enhanced in human lung cancer (Jala, et al. 2012). Altogether, these data indicate that the
128 molecular pathways sustaining the impact of sex and of estrogen pathway on lung cancer cell
129 growth and more specifically on lung cancer lymphangiogenesis and angiogenesis are still
130 insufficiently understood.

131 In this study, we report that the sex of lung microenvironment affects lung tumour
132 development. Orthotopically grafting syngeneic lung cancer cells into pulmonary parenchyma
133 of immunocompetent mice revealed that lung tumours grew faster in female mice than in
134 males. E2 increased tumour progression in female mice and enhanced lymphangiogenesis and
135 angiogenesis through an ER α -dependent pathway. Furthermore, while treatment with ER β
136 antagonist was inefficient, treatment by ER α antagonist and tamoxifen decreased lung tumour
137 growth in females but not in males. Finally, lymphangiogenesis and angiogenesis were higher
138 in lung adenocarcinoma samples issued from young women as compared to those obtained
139 from young men.

140

141 **Materials & Methods**

142 *Human samples and ethical study approval*

143 Human lung tumour samples, endometrium and testis tissues were provided by the Biobank of
144 the University Hospital of Liège (BHUL, University of Liège and CHU of Liège, Belgium) to
145 perform a retrospective study in accordance with the current legislation and recommendations
146 of the Ethical Committee of the University Hospital of Liège.

147 *Animals and ethical study approval*

148 C57BL/6J mice were purchased from Charles River (France). Tie2-Cre⁺/ERa^{lox/lox} mice and
149 their control littermates Tie2-Cre⁻/ERa^{lox/lox} in C56BL/6J background were generated as
150 described previously (Billon-Gales, et al. 2009). Mouse genotyping is provided in
151 Supplementary Fig.1. All animals were maintained within the accredited Mouse Facility and
152 Transgenics GIGA platform of the University of Liège (Belgium). All animal experiments
153 were conducted in accordance with the Federation of European Laboratory Animal Science
154 Associations (FELASA) and were approved by the local ethical committee of the University
155 of Liège.

156 *Reagents*

157 E2 was purchased from Sigma-Aldrich. MPP dihydrochloride (1.3-bis(4-hydroxyphenyl)-4-
158 methyl-5-(4-(2-piperidinyloxy)phenol)-1H-pyrazole dihydrochloride); PHTPPP (4-(2-
159 phenyl-5,7-bis(trifluoromethyl)pyrazolo(1,5-a)pyrimidin-3-yl)phenol)) and G15
160 ((3aS*,4R*,9bR*)-4-(6-Bromo-1,3-benzodioxol-5-yl)-3a,4,5,9b-3H-cyclopenta[c]quinoline)
161 were purchased from Tocris Biosciences (R&D system, Abingdon, UK).

162 *Cell cultures*

163 MCF-7 cells (HTB-22™) and male mouse Lewis Lung Carcinoma cells transfected with
164 luciferase gene (LLC-Luc, LL/2-luc-M38) were purchased from American Type Culture
165 Collection (ATCC, Manassas, VA, USA) and Caliper Lifesciences (Hopkinton, MA, USA),
166 respectively. MCF-7 and LLC-Luc cells were authenticated by Leibniz-Institute DSMZ using
167 STR DNA typing and Cytochrome Oxidase subunit 1 (COI) alignment respectively. All cells
168 were used within 10 passages after authentication. Cells were routinely cultured in DMEM
169 (Gibco Invitrogen Corporation, Paisley, United Kingdom) supplemented with 10% heat-
170 inactivated foetal bovine serum (FBS, Lonza, Basel, Switzerland), 2 mM glutamine and 100
171 UI/ml penicillin/streptomycin (ThermoFisher Scientific, MA, USA).

172 *Cell proliferation and viability assays*

173 LLC-Luc cells were cultured for 24h in red phenol-free medium (Gibco Invitrogen
174 Corporation, Paisley, UK) supplemented with 10% of heat-inactivated and dextran-coated
175 charcoal treated foetal bovine serum (FBS-cs, Lonza, Basel, Switzerland). Cells were then
176 cultured in medium with 2% FBS-cs supplemented with either 10% FBS (positive control) or
177 E2 (10^{-10} M to 10^{-7} M) or MPP (10^{-8} M) or PHTPP (10^{-8} M) or G15 (10^{-7} M) or vehicle (DMSO
178 0.001%) or cisplatin as positive control (100 μ M, #P4394, Sigma-Aldrich, St-Louis, MO,
179 USA). To investigate cell proliferation, LLC-Luc cells were incubated during 24h with
180 methyl-³[H]thymidine (Perkin Elmer Life Sciences, Boston, MA, USA) and radioactivity was
181 measured with a b-counter (Beckman, LS-5000-CE); to measure cell viability, an MTT test
182 (#11465007001, Roche, Basel, Switzerland) was performed in accordance with
183 manufacturer's instructions.

184 *Western Blotting*

185 Mouse testis and ovary tissues were collected as described below. Cells and tissues were
186 lysed in RIPA buffer supplemented with a protease inhibitor (Complete, Roche, Basel,
187 Switzerland). Primary antibodies used for immunostaining were anti-ERa (clone 60C, #04-
188 820, Millipore; F10, #sc-8002, Santa Cruz, CA, USA), anti-ERb (PPZ0506, #417100,
189 Invitrogen/ThermoFisher Scientific, MA, USA), anti-GPER (#sc-48525, Santa Cruz, CA,
190 USA) and anti-HSC70 (B-6, #sc-7298, Santa Cruz, CA, USA). After incubation with
191 appropriated HRP-conjugated secondary antibodies, immunoreactions were revealed using
192 the enhanced chemoluminescence kit (Thermofisher Scientific, MA, USA). Images were
193 acquired by a LAS4000 digital camera (FujiFilm, Japan).

194 *Mouse orthotopic model of lung cancer*

195 When required by the experimental protocol, five weeks old mice were gonadectomised.
196 Ovaries and testis tissues were collected as control samples for western blot assays. Two

197 weeks after surgery, some females were treated with subcutaneous slow-releasing E2 pellets
198 (OVX+E2) (75µg/kg/day, #ME2-60 days, Belma Technologies, Belgium) (Gerard, et al.
199 2017). Ten days later, LLC-Luc cells (2×10^6 cells/mice) were instilled into lungs as
200 previously described (Rocks, et al. 2012). For ER antagonist treatments, mice were either
201 subcutaneously injected with MPP, PHTPP (1mg/kg in peanut oil) or DMSO (vehicle, 5% in
202 peanut oil) 5 days a week; or received a subcutaneous pellet of tamoxifen (5mg/60days
203 release, Innovative Research of America, FL, USA). All treatments were started 2 weeks
204 before the LLC-Luc cell instillation and were conducted until sacrifice at day 21 after tumour
205 cell instillation. To monitor lung tumour growth, luciferin (150mg/kg in PBS, #E160E,
206 Promega, WI, USA) was injected intraperitoneally and luciferase bioluminescence was
207 measured using the bioluminescent IVIS imaging system (Xenogen-Caliper, Hopkinton, MA,
208 USA).

209 *Lung tumour immunohistochemical analysis*

210 To evaluate tumour density, paraffin-embedded lung tumour sections (5µm) were stained
211 with hematoxylin and eosin (H/E). For each mouse, we collected 8 slides separated by 50 µm.
212 Numeric images were obtained with NanoZoomer 2.0-digital slide scanner (Hamamatsu
213 Photonics, Japan). On each slide, the lung tumour area and the total lung area were measured
214 by computer assisted image analysis with Matlab software (MathWorks, Inc., MA, USA). The
215 ratio of these two measures (lung tumour area/total lung area) correspond to the lung tumour
216 density. To obtain the lung tumour density for one mouse, we calculated the mean of the 8
217 densities measured from the 8 slides of the same lung.

218 Immunolabelings were carried out using anti-CD31 (#ab28364, Abcam, Cambridge, United
219 Kingdom), anti-podoplanin (D2-40, #MA1-83884, Thermofisher Scientific, MA, USA), anti-
220 LYVE1 (#AF2125, R&D System, Abingdon, UK) or anti-ERα (1D5, #M7047, Dako,
221 Glostrup, Denmark) antibodies. Slides were then incubated with appropriate biotin-coupled

222 secondary antibodies (Dako, Glostrup, Denmark) and with streptavidin/alexa 555 or
223 streptavidin/Alexa 488 (#S21381, #A11055, Invitrogen Corporation, Paisley, UK). Slides
224 were mounted with DAPI fluoromount G (SouthernBiotech, AL, USA). Numeric images were
225 obtained with NanoZoomer 2.0-digital slide scanner (Hamamatsu Photonics, Japan) or
226 recorded with fluorescence microscope (VANOX AHBT3, Olympus, Belgium). For each
227 mouse tumour sample, a minimum of 5 optical fields that cover the entire tumour section
228 were recorded and a mean density was calculated. Lymphangiogenesis and angiogenesis
229 densities were quantified as a ratio between the area occupied by LYVE1, PDPN or CD31
230 staining in the tumour and the area of the tumour. Image analysis was performed with Matlab
231 software (MathWorks, Inc, MA, USA) as previously described (Pequeux, et al. 2012).

232 *EdU incorporation assay*

233 Two hours before sacrifice, mice received a peritoneal injection of 5-ethynyl-2'-deoxyuridine
234 (EdU, 2.5mg/mouse, ThermoFisher Scientific, MA, USA). EdU incorporation in proliferating
235 cells was evidenced using Click-it EdU cocktail kit (Molecular Probes, Merelbeke, Belgium)
236 in accordance with manufacturer's instructions. Slides were mounted with aquapolymount
237 (Polysciences, Hirschberg an der Bergstrasse, Germany).

238 *Corneal assay*

239 The ophthalmic cauterization of cornea was performed and analysed, as previously described
240 (Detry, et al. 2013). Briefly, mice were anesthetized with ketamine hydrochloride (100 mg/kg
241 body weight) and xylazine (10 mg/kg body weight) by peritoneal injection; their eyes were
242 locally anesthetized with Unicaïne 0.4% drops (Thea Pharma, Wetteren, Belgium). After
243 anaesthesia, an ophthalmic cauterization (Optemp II V; Alcon Surgical, Fort Worth, TX,
244 USA) was performed in the central part of the cornea. Corneas were recovered and they were
245 dissected at day 7 post-injury. Tissue was fixed during 1 hour in 70% ethanol at room
246 temperature, washed in PBS and blocked during 1 hour in milk3%/BSA3% (Nestlé, Brussels,

247 Belgium; Acros Organics, NJ, USA). To highlight lymphatic and blood vessels, tissues were
248 first incubated overnight with polyclonal goat anti-mouse LYVE1 (1:200, #AF2125, R&D
249 system, Abingdon, UK) and monoclonal rat anti-mouse CD31 (1:200, #01951D, BD
250 Biosciences Pharmingen, San Jose, CA, USA), then with rabbit anti-goat/Alexa Fluor 488
251 (1:200, #A21222, Molecular Probes, Merelbeke, Belgium) or goat anti-rat/Alexa Fluor 546
252 (1:200, #A11035, Molecular Probes, Merelbeke, Belgium) antibodies, respectively. Corneas
253 were whole-mounted with Vectashield (Vector Laboratories, Burlingame, CA, USA) and
254 pictures were acquired with FSX100 microscope (Olympus, Japan). These experiments were
255 performed on males, females, gonadectomised-mice and ovariectomised female mice treated
256 with subcutaneous slow-releasing E2 pellets (75µg/kg/day, #ME2-60 days, Belma
257 Technologies, Liège, Belgium). This cornea assay was also carried out on female mice treated
258 with subcutaneous injections of MPP, PHTPP or with G15 (1mg/kg/day, Tocris Biosciences,
259 R&D system, Abingdon, UK) for 3 weeks (5 times/week). These treatments started 2 weeks
260 before thermal cauterization until sacrifice.

261 *Protein quantification by Milliplex assay*

262 Proteins from LLC-Luc lung tumours were extracted and analysed by Milliplex assay of
263 mouse angiogenesis/growth factor, accordingly to manufacturer's instructions (Mouse
264 Angiogenesis/Growth Factor Magnetic Bead Panel – Cancer Mutliplex Assay #MAGPMAG-
265 24K, Merck, Darmstadt, Germany).

266 *RNA in situ hybridization (RNAscope)*

267 The mRNA in situ hybridization of ERα (ESR1), CD31 (PECAM) and podoplanin (PDPN)
268 was measured on human lung tumour (men and women) and endometrium tissue sections
269 with the RNAscope assay (Advanced Cell Diagnostics, Bioké, Leiden, The Netherlands)
270 according to manufacturer's instructions. Briefly, paraffin-embedded tissue sections (5µm)
271 were deparaffinized and hybridized in duplex, either with Hs-ESR1 (#310301, Bioké, Leiden,

272 The Netherlands) and Hs-PECAM1-O1-C2 (#487381-C2, Bioké, Leiden, The Netherlands)
273 probes or with Hs-ESR1 (#310301, Bioké, Leiden, The Netherlands) and Hs-PDPN-C3
274 (#539751-C3, Bioké, Leiden, The Netherlands) probes or with RNAscope 3-plex negative
275 control probe (#320871, Bioké, Leiden, The Netherlands). Hybridization signal was amplified
276 with RNAscope Multiplex Fluorescent reagent kit V2 (#323100, Bioké, Leiden, The
277 Netherlands) and TSA Plus Fluorescent kits (#NEL745001KT, #NEL744001KT,
278 PerkinElmer, MA, USA). Images were recorded with a confocal Olympus Fluoview 1000
279 microscope (Olympus America, Waltham, MA, USA) at 40X of magnification.

280 *Statistical analysis*

281 Results were were analysed with GraphPad Prism 5.0 (San Diego, CA, USA). Statistical
282 analyses were assessed with Student t-test or One-way ANOVA followed by Bonferroni post-
283 test for Gaussian distribution, with Mann-Whitney or Kruskal-Wallis for non-Gaussian
284 distribution and with Two-way ANOVA for grouped analysis. Mann-Whitney was also used
285 to compare independent experimental groups. The p value was expressed as followed:
286 * $p < 0.05$; ** $p < 0.01$; *** $p < 0.001$.

287

288 **Results**

289 ***Female mice develop larger lung tumours than males, through an E2-dependent pathway***

290 To understand the impact of sex on lymphangiogenic and angiogenic processes associated to
291 lung adenocarcinoma development, we used an orthotopic syngeneic lung cancer model,
292 which was developed in immunocompetent mice in order to preserve the integrity of the lung
293 microenvironment.

294 Twenty-one days after intratracheal LLC-Luc administration, bioluminescent signals
295 produced by lung tumours were higher in females as compared to males (Fig. 1A).
296 Quantification of tumour area on histological lung sections confirmed that females developed

297 approximately 2-fold larger lung tumours than males (Fig. 1B). To evaluate the effects of
298 endogenous estrogen in sex-related differences regarding lung tumour development, females
299 were ovariectomised (OVX) and LLC-Luc tumour implantation in lung parenchyma was
300 measured. Interestingly, OVX female mice displayed a decreased lung tumour growth as
301 compared to naive females and to OVX females supplemented with exogenous E2 (OVX+E2)
302 (Fig. 1C-D). By contrast, lung tumour growth was not affected by gonadectomy in males,
303 even after E2 supplementation (Fig. 1E-F). This suggests a specific effect of endogenous and
304 exogenous estrogens on tumour growth in female lungs but not in males.

305 ***E2 increases LLC-Luc cell proliferation in vivo but not in vitro***

306 LLC-Luc cells used in the orthotopic lung cancer model expressed GPER, but not ERa
307 receptor (Fig. 2A). ERb expression was assessed using the anti-ERb antibody PPZ0506, the
308 only specific and commercially available antibody validated by Andersson *et al* (Andersson,
309 *et al. 2017*). No expression of ERb was detected in LLC-Luc protein extracts.

310 Treatment of LLC-Luc cells with increasing E2 concentrations, ranging from 10^{-10} M to 10^{-7}
311 M, for 24, 48 or 72 hours did neither affected LLC-Luc proliferation (Fig. 2B-C) nor cell
312 viability (Fig. 2D). FBS and cisplatin were used as positive and negative controls in the
313 proliferation or viability assays, respectively. In addition, the combined treatment of cells
314 with E2 and ER antagonists, MPP (ERa antagonist), PHTPP (ERb antagonist) or G15 (GPER
315 antagonist), did not modulate cell proliferation (Fig. 2E). These results highlight that E2 does
316 not directly increase lung cancer cell proliferation, despite GPER expression by those cells.

317 To assess LLC-Luc cell proliferation *in vivo*, tumour-bearing mice were intraperitoneally
318 injected with EdU (Fig. 2F). Interestingly, EdU density was higher in LLC-Luc lung tumours
319 when OVX mice were treated with E2 (OVX+E2) (Fig. 2G). In these tumours, the expression
320 of ERa by cancer cells was not induced *in vivo* (Fig. 2H-I). However, some positivity was

321 associated to lymphatic and blood vessels, as shown by co-immunostainings (yellow staining,
322 white arrows) of ER α and LYVE1 (Fig. 2G) or CD31 (Fig. 2H).

323 Altogether, these results highlight that when lung cancer cells do not express ERs, E2 can still
324 promote lung tumour growth *in vivo*.

325 ***E2 increases lymphangiogenesis and angiogenesis in females***

326 A significant higher lymphatic vessel density was detected in tumours grown in female lungs
327 as compared to male counterparts (Fig. 3A-B). While ovariectomy (OVX) decreased tumour
328 lymphatic vessel density, E2 supplementation of OVX mice (OVX+E2) was able to rescue it.
329 In male mice, there was no effect of castration and E2 treatment on lung tumour
330 lymphangiogenesis. Similarly to lymphatic vessel, blood vessel density was increased in lung
331 tumours grown in female mice (Fig. 3A-B). Furthermore, when OVX females were used, E2
332 treatment increased tumour-related blood vessel network, while no modulation was observed
333 in males. VEGFC, VEGFD, VEGFA and bFGF, the main prolymphangiogenic and
334 proangiogenic factors, were measured by Milliplex assay in lung tumour samples. VEGFC
335 and VEGFD levels were not modulated between experimental groups (Fig. 3C-D). VEGFA
336 and bFGF levels were increased in LLC-Luc lung tumours grown in females as compared to
337 males and in OVX females treated with E2 as compared to OVX mice (Fig. 3E-F).

338 In order to evaluate if vascular modulation by E2 was only related to lung tumour-associated
339 processes or if it could be extended to other pathological lymphangiogenic and angiogenic
340 processes, a model of cornea injury was used to concomitantly study lymphangiogenic and
341 angiogenic response in an inflammatory context (Detry et al. 2013). In this model, OVX
342 females displayed decreased lymphatic and blood vessel densities, which were restored upon
343 E2 supplementation (OVX+E2) (Fig. 3G). Castration (Cx) of males did not modulate neither
344 lymphangiogenesis nor angiogenesis (Fig. 3H).

345 Altogether, these results show that E2 promotes pathological lymphangiogenesis and
346 angiogenesis only in females and increases VEGFA and bFGF in lung tumours.

347 ***Prolymphangiogenic and proangiogenic effects of E2 are mediated by ERa***

348 To define whether ERa signalling contributes to the sex-dependent control of
349 lymphangiogenesis and angiogenesis in lung cancer, the impact of ERa deletion in lymphatic
350 and blood endothelial cells was evaluated by performing experiments in Tie2-Cre/ERa^{lox/lox}
351 mice.

352 When compared to males, the increase of lung tumour growth observed in female control
353 Tie2-Cre⁻/ERa^{lox/lox} mice was inhibited in Tie2-Cre⁺/ERa^{lox/lox} mice (Fig. 4A). In addition, the
354 increase of lung tumour growth induced by E2 in OVX female control Tie2-Cre⁻/ERa^{lox/lox}
355 mice was abrogated in Tie2-Cre⁺/ERa^{lox/lox} mice (Fig. 4B).

356 Quantification of the lymphatic and blood vessel networks in tumours that grew in Tie2-
357 Cre⁺/ERa^{lox/lox} mice (ERa-deficiency in vessels) did not show any statistical variation between
358 the four aforementioned experimental groups (Fig. 4C-D). Moreover, by applying the model
359 of cornea injury to these Tie2-Cre⁺/ERa^{lox/lox} mice, we did not observe any difference of
360 lymphangiogenesis and angiogenesis responses between the experimental groups (Fig. 4E).
361 To evaluate the potential contributions of the other estrogen receptors, we tested
362 pharmacological inhibitors of ERa (MPP), ERb (PHTPP) and GPER (G15) on the cornea
363 injury model in wild-type female mice. MPP decreased both corneal lymphangiogenesis and
364 angiogenesis confirming ERa signalling involvement (Fig. 4F). However, PHTPP and G15
365 did not exert any effect on lymphatic and blood vessel networks.

366 Altogether, these results support that ERa is the unique estrogen receptor that mediates E2
367 effects on lymphangiogenesis and angiogenesis.

368 ***Treatment with ERa antagonists inhibits lung tumour growth, lymphangiogenesis and***
369 ***angiogenesis in females, but not in males***

370 LLC-Luc tumour growth was evaluated in females and males treated with MPP (ERa
371 antagonist), PHTPP (ERb antagonist) or tamoxifen (Tmx), an ER antagonist widely used in
372 female patients suffering from hormone-dependent breast cancer (Early Breast Cancer
373 Trialists' Collaborative, et al. 2011). In female animals, both MPP and tamoxifen decreased
374 tumour growth, while PHTPP was not efficient (Fig. 5A-B). In addition, females treated with
375 MPP or tamoxifen presented reduced tumour lymphatic or blood vessel networks when
376 compared to control mice treated with vehicle (Fig. 5C-D). No modulation was observed in
377 vessels when mice were treated with PHTPP (Fig. 5C-D). Levels of VEGFC and VEGFD
378 were not modified in these experimental conditions (Fig 5E-F). In contrast, treatment with
379 MPP or tamoxifen decreased VEGFA and bFGF levels measured in lung tumours from
380 females (Fig. 5G-H), while PHTPP had no effect (Supplementary Fig.2).

381 In males, none of the used antagonists (MPP, PHTPP, tamoxifen) was able to modulate LLC-
382 Luc tumour development (Fig. 5I-J), lymphangiogenesis (Fig. 5K) or angiogenesis (Fig. 5L).
383 These results show sex specific reactivity towards treatments targeting ERa signalling.

384 ***Lymphangiogenesis and angiogenesis rates are higher in lung adenocarcinoma samples of***
385 ***women than men***

386 To validate the clinical relevance of our findings, we measured lymphatic and blood vessel
387 densities on human lung cancer biopsies and evaluated if lymphangiogenesis and
388 angiogenesis were differentially regulated in lung cancer developing in women or in men. For
389 this retrospective study, a cohort of patients with lung cancer (n=74) and aged between 35 to
390 55 years old has been selected to ensure that lung carcinogenesis had occurred before
391 menopause (Fig. 6A). Although the mean age was similar for both experimental groups and
392 all subjects included in this study were smokers, except one woman, one noteworthy data is
393 that almost twice more biopsies were available from women (n=51) than from men (n=23)
394 (Fig. 6A). Similar percentage of cancer cells positive for ERa was detected in man (60.9%)

395 and in woman (62.7%) samples as assessed by nuclear immunohistochemical staining (Fig.
396 6B).

397 Podoplanin (PDPN) staining on tissue samples of lung adenocarcinoma showed that
398 lymphangiogenesis was higher in women than men, independently of ER α status in cancer
399 cells (Fig. 6C). CD31 staining showed that angiogenesis was higher in ER-negative lung
400 adenocarcinoma from women, when patient cohorts were selected by ER α status (Fig. 6D). In
401 addition, we evidenced by RNAscope methodology that ER α mRNA was expressed by CD31-
402 and PDPN-positive cells (Fig. 6E) of these lung adenocarcinoma sections.

403 **Discussion**

404 This study highlights the contribution of lymphatic and blood endothelia in the sex-dependent
405 modulation of lung cancer progression. Based on histological analysis of human lung
406 adenocarcinoma samples and on experimental *in vivo* models, our study shows that the
407 “female microenvironment” offers a better soil for lung tumour development. Notably,
408 estrogens in females promote lymphangiogenesis and angiogenesis in an ER α -dependent
409 manner. This new original concept is supported by drastic reduction of lymph/angiogenesis
410 and tumour growth upon treatment with pharmacological ER α antagonist and tamoxifen,
411 which showed efficacy only in females but not in males.

412 Several preclinical and clinical studies reported a positive correlation between estrogens and
413 lung tumour growth, especially through a direct action on ER-positive cancer cells
414 (Hammoud et al. 2008; Liu, et al. 2015; Mah et al. 2007; Tang et al. 2014). The originality of
415 this study is to highlight that sex and estrogenic status of the host lung parenchyma regulates
416 the development of lung adenocarcinoma cells by modulating lymphangiogenesis and
417 angiogenesis. Our results are in accordance with reviews highlighting underappreciated sex
418 differences in vascular physiology and pathophysiology (Boese, et al. 2017; Stanhewicz, et al.
419 2018). Angiogenesis is one of the leading processes that support cancer development allowing

420 the tumours to be fuelled with oxygen and nutrients (De Palma et al. 2017). Tumour-
421 associated lymphangiogenesis more recently emerged as an active player and a novel
422 potential therapeutic target, due to its contribution (1) in antigen, fluid and metastatic cell
423 transport, (2) in the regulation of cancer stemness and (3) in immunomodulation (Dieterich
424 and Detmar 2016; Paupert et al. 2011; Petrova and Koh 2018).

425 A key finding is that lymph/angiogenesis was markedly higher in lung adenocarcinoma of
426 woman patients than men, especially when cancer cells did not express ERa, although ERa is
427 expressed by lymphatic and blood endothelial cells. We applied an orthotopic syngeneic
428 model of lung cancer in immunocompetent mice lacking ERa in Tie2-positive cells (Tie2-
429 Cre⁺/ERa^{lox/lox}) and therefore in lymphatic and blood endothelium (Billon-Gales et al. 2009;
430 Kisanuki, et al. 2001; Morfoisse, et al. 2018). Through this genetic approach, we delineated
431 that ERa signalling mediates an E2-dependent lung tumour lymph/angiogenesis in females,
432 while ERb and GPER are not involved. Our results are in line with studies reporting that
433 major E2-related blood endothelial functions are mediated through ERa (Billon-Gales et al.
434 2009; Brouchet, et al. 2001; Guivarc'h, et al. 2018; Kim, et al. 2014; Pequeux et al. 2012).
435 Although ERa signalling has been recently reported to mediate E2 protective effects on
436 secondary lymphedema (Morfoisse et al. 2018), the contribution of E2/ERa signalling to
437 tumour lymphangiogenesis had not been reported yet. In line with our data,
438 lymphangiogenesis was also increased in the heart of mouse after myocardial infarction when
439 cardiomyocytes overexpressed ERa (Mahmoodzadeh, et al. 2014). Interestingly, the
440 prolymphangiogenic effect of the E2/ERa pathway that we observed on lung tumour
441 lymphangiogenesis in females could also be extended to inflammatory-related
442 lymphangiogenesis. Indeed, the use of Tie2-Cre⁺/ERa^{lox/lox} mice or treatment of wild-type
443 mice with a pharmacological inhibitor of ERa prevented lymphangiogenesis in the cornea
444 injury assay. Altogether, these results support a significant contribution of E2/ERa signalling

445 in regulation of lymphatic and blood endothelia functions under pathological conditions.

446 For the first time, we demonstrate the regulation of lymph/angiogenesis by E2/ERa signalling
447 in lung cancer. We delineate that endogenous or exogenous E2 contributes to increase
448 lymph/angiogenesis and levels of VEGFA and bFGF in lung tumours of females. This is in
449 line with previous reports showing an E2-dependent upregulation of VEGFA and bFGF in
450 several tissues (Garmy-Susini, et al. 2004; Pequeux et al. 2012) and with the ERa-dependent
451 upregulation of VEGFR2 observed in myometrial and retinal microvascular endothelial cells
452 treated with E2 (Gargett, et al. 2002; Suzuma, et al. 1999). While VEGFA overexpression is
453 correlated with a poor prognosis in lung cancer patients, VEGFC levels are not associated
454 with survival (Zhan, et al. 2009). In the same model, lymphangiogenesis was not increased
455 through VEGFC or VEGFD overexpression, but was correlated with an increase of VEGFA
456 and bFGF levels. Although the action of VEGFC and VEGFD on VEGFR3 is the major
457 pathway for lymphangiogenesis promotion (Alitalo and Detmar 2012; Zhang, et al. 2010),
458 VEGFA and bFGF were also described to stimulate this process (Cao, et al. 2012; Cursiefen,
459 et al. 2004; Detry et al. 2013). Especially, bFGF has been described to interact with VEGFC
460 and to collaboratively promote tumour growth, lymphangiogenesis and metastasis in an
461 experimental mouse model of fibrosarcoma (Cao et al. 2012). These data suggest that the
462 increase of bFGF observed in females and E2-treated mice could reinforce the action of
463 VEGFC to increase lymphangiogenesis even if VEGFC levels are not directly modulated.

464 Since the female microenvironment of lung tumours appeared to be more sensitive to
465 estrogens through ERa signalling, female mice were treated with an ERa antagonist or with
466 tamoxifen, an anti-estrogen therapy largely used in breast cancer patients. Interestingly, ERa
467 antagonist or tamoxifen decreased lung tumour growth and lymph/angiogenesis.
468 Concomitantly, these treatments also reduced VEGFA and bFGF, but not VEGFC and
469 VEGFD levels. These observations corroborate clinical data showing that tamoxifen

470 decreases lung cancer probability in patients (Bouchardy et al. 2011; Chu et al. 2017).
471 Tamoxifen also prevents the protective effect of E2 on secondary lymphedema (Morfoisse et
472 al. 2018). In addition, tamoxifen can also reduce capillary tube formation and endothelial cell
473 migration by decreasing platelet-related VEGFA discharge (Johnson, et al. 2017). More
474 interestingly, these treatments failed to impact lung tumour growth and lymph/angiogenesis in
475 males. Our results thus provide an explanation for the sex specificities evidenced in lung
476 cancer patients, where young women (30-39 years old) display higher lung cancer incidence
477 than young men (Jemal et al. 2018).

478 In summary, this study emphasizes that female microenvironment sustains more efficiently
479 lung tumour development than the male one. Especially, estrogens increase
480 lymph/angiogenesis through an ERa-dependent pathway. In accordance, treatment by ERa
481 antagonist or tamoxifen decreases lung tumour growth and lymph/angiogenesis in females but
482 not in males.

483 In addition to shedding light on sex issues in lung cancer in young patients, our study has
484 potential clinical implication by pointing to the importance of estrogen status or
485 supplementation on lung cancer development that should be considered to adapt therapeutic
486 strategies.

487 **Conflict of interest statement:** The authors have nothing to disclose.

488

489 **Funding**

490 This work was supported by grants from the Fonds de la Recherche Scientifique – FNRS-
491 Télévie (F.R.S.-FNRS, Belgium), the Fondation contre le Cancer (foundation of public
492 interest, Belgium), the Fonds spéciaux de la Recherche (University of Liège), the Centre
493 Anticancéreux près l'Université de Liège, the Fonds Léon Fredericq (University of Liège), the

494 Direction Générale Opérationnelle de l'Economie, de l'Emploi et de la Recherche (DGO6,
495 SPW, Belgium).

496

497 **Author Contribution**

498 C.D. performed the experiments and prepared the figures and the manuscript. N.R. developed
499 the *in vivo* model of lung cancer, gave scientific advices along the study and critically
500 reviewed the manuscript. S.B. developed and performed all computer assisted quantification
501 analysis. I.P., A.G. and M.G-C contributed to *in vitro* and *in vivo* experiments and critically
502 reviewed the manuscript. L.B. supported the study with critical clinical advices. A.G.
503 supported the study with scientific advices all along the study and critically discussed study
504 design and manuscript. F.L. contributed to the genesis of the project, supported the study with
505 scientific advices along the study and critically reviewed the manuscript. D.C. supervised the
506 project, was responsible for finding funding and critically reviewed the manuscript. C.P.
507 initiated and supervised the project, was responsible for finding funding, designed the
508 experiments, analysed data and wrote the manuscript.

509

510 **Acknowledgments**

511 We thank the GIGA-Imaging and Flow Cytometry platform and the GIGA-Mouse facility
512 platform (GIGA, University of Liège). We thank Isabelle Dasoul, Marie Dehuy, Emilie
513 Feyereisen, Christine Fink, Pascale Heneaux, Erika Konradowski, Fabienne Perin and Céline
514 Vanwinge for their excellent technical assistance.

515

516 **References**

517 Alitalo A & Detmar M 2012 Interaction of tumor cells and lymphatic vessels in cancer
518 progression. *Oncogene* **31** 4499-4508.
519 Alitalo K, Tammela T & Petrova TV 2005 Lymphangiogenesis in development and
520 human disease. *Nature* **438** 946-953.

- 521 Andersson S, Sundberg M, Pristovsek N, Ibrahim A, Jonsson P, Katona B, Clausson CM,
522 Zieba A, Ramstrom M, Soderberg O, et al. 2017 Insufficient antibody validation
523 challenges oestrogen receptor beta research. *Nat Commun* **8** 15840.
- 524 Baik CS & Eaton KD 2012 Estrogen signaling in lung cancer: an opportunity for novel
525 therapy. *Cancers* **4** 969-988.
- 526 Barton M, Filardo EJ, Lolait SJ, Thomas P, Maggiolini M & Prossnitz ER 2017 Twenty
527 years of the G protein-coupled estrogen receptor GPER: Historical and personal
528 perspectives. *J Steroid Biochem Mol Biol*.
- 529 Billon-Gales A, Fontaine C, Douin-Echinard V, Delpy L, Berges H, Calippe B, Lenfant F,
530 Laurell H, Guery JC, Gourdy P, et al. 2009 Endothelial estrogen receptor-alpha plays a
531 crucial role in the atheroprotective action of 17beta-estradiol in low-density lipoprotein
532 receptor-deficient mice. *Circulation* **120** 2567-2576.
- 533 Boese AC, Kim SC, Yin KJ, Lee JP & Hamblin MH 2017 Sex differences in vascular
534 physiology and pathophysiology: estrogen and androgen signaling in health and disease.
535 *Am J Physiol Heart Circ Physiol* **313** H524-H545.
- 536 Bouchardy C, Benhamou S, Schaffar R, Verkooijen HM, Fioretta G, Schubert H, Vinh-Hung
537 V, Soria JC, Vlastos G & Rapiti E 2011 Lung cancer mortality risk among breast cancer
538 patients treated with anti-estrogens. *Cancer* **117** 1288-1295.
- 539 Brouchet L, Krust A, Dupont S, Chambon P, Bayard F & Arnal JF 2001 Estradiol
540 accelerates reendothelialization in mouse carotid artery through estrogen receptor-
541 alpha but not estrogen receptor-beta. *Circulation* **103** 423-428.
- 542 Cadranel J, Zalcman G & Sequist L 2011 Genetic profiling and epidermal growth factor
543 receptor-directed therapy in nonsmall cell lung cancer. *Eur Respir J* **37** 183-193.
- 544 Cao R, Ji H, Feng N, Zhang Y, Yang X, Andersson P, Sun Y, Tritsarlis K, Hansen AJ, Dissing S,
545 et al. 2012 Collaborative interplay between FGF-2 and VEGF-C promotes
546 lymphangiogenesis and metastasis. *Proc Natl Acad Sci U S A* **109** 15894-15899.
- 547 Chlebowski RT, Wakelee H, Pettinger M, Rohan T, Liu J, Simon M, Tindle H, Messina C,
548 Johnson K, Schwartz A, et al. 2016 Estrogen Plus Progestin and Lung Cancer: Follow-up
549 of the Women's Health Initiative Randomized Trial. *Clin Lung Cancer* **17** 10-17 e11.
- 550 Chu SC, Hsieh CJ, Wang TF, Hong MK & Chu TY 2017 Antiestrogen use in breast cancer
551 patients reduces the risk of subsequent lung cancer: A population-based study. *Cancer*
552 *Epidemiol* **48** 22-28.
- 553 Cursiefen C, Chen L, Borges LP, Jackson D, Cao J, Radziejewski C, D'Amore PA, Dana MR,
554 Wiegand SJ & Streilein JW 2004 VEGF-A stimulates lymphangiogenesis and
555 hemangiogenesis in inflammatory neovascularization via macrophage recruitment. *J Clin*
556 *Invest* **113** 1040-1050.
- 557 De Palma M, Biziato D & Petrova TV 2017 Microenvironmental regulation of tumour
558 angiogenesis. *Nat Rev Cancer* **17** 457-474.
- 559 Detry B, Blacher S, Erpicum C, Paupert J, Maertens L, Maillard C, Munaut C, Sounni NE,
560 Lambert V, Foidart JM, et al. 2013 Sunitinib inhibits inflammatory corneal
561 lymphangiogenesis. *Invest Ophthalmol Vis Sci* **54** 3082-3093.
- 562 Dieterich LC & Detmar M 2016 Tumor lymphangiogenesis and new drug development.
563 *Adv Drug Deliv Rev* **99** 148-160.

- 564 Early Breast Cancer Trialists' Collaborative G, Davies C, Godwin J, Gray R, Clarke M,
565 Cutter D, Darby S, McGale P, Pan HC, Taylor C, et al. 2011 Relevance of breast cancer
566 hormone receptors and other factors to the efficacy of adjuvant tamoxifen: patient-level
567 meta-analysis of randomised trials. *Lancet* **378** 771-784.
- 568 Gargett CE, Zaitseva M, Bucak K, Chu S, Fuller PJ & Rogers PA 2002 17Beta-estradiol up-
569 regulates vascular endothelial growth factor receptor-2 expression in human
570 myometrial microvascular endothelial cells: role of estrogen receptor-alpha and -beta. *J*
571 *Clin Endocrinol Metab* **87** 4341-4349.
- 572 Garmy-Susini B, Delmas E, Gourdy P, Zhou M, Bossard C, Bugler B, Bayard F, Krust A,
573 Prats AC, Doetschman T, et al. 2004 Role of fibroblast growth factor-2 isoforms in the
574 effect of estradiol on endothelial cell migration and proliferation. *Circ Res* **94** 1301-1309.
- 575 Gerard C, Gallez A, Dubois C, Drion P, Delahaut P, Quertemont E, Noel A & Pequeux C
576 2017 Accurate Control of 17beta-Estradiol Long-Term Release Increases Reliability and
577 Reproducibility of Preclinical Animal Studies. *J Mammary Gland Biol Neoplasia* **22** 1-11.
- 578 Greiser CM, Greiser EM & Doren M 2010 Menopausal hormone therapy and risk of lung
579 cancer-Systematic review and meta-analysis. *Maturitas* **65** 198-204.
- 580 Guivarc'h E, Buscato M, Guihot AL, Favre J, Vessieres E, Grimaud L, Wakim J, Melhem NJ,
581 Zahreddine R, Adlanmerini M, et al. 2018 Predominant Role of Nuclear Versus
582 Membrane Estrogen Receptor alpha in Arterial Protection: Implications for Estrogen
583 Receptor alpha Modulation in Cardiovascular Prevention/Safety. *J Am Heart Assoc* **7**.
- 584 Hamilton KJ, Hewitt SC, Arao Y & Korach KS 2017 Estrogen Hormone Biology. *Curr Top*
585 *Dev Biol* **125** 109-146.
- 586 Hammoud Z, Tan B, Badve S & Bigsby RM 2008 Estrogen promotes tumor progression in
587 a genetically defined mouse model of lung adenocarcinoma. *Endocr Relat Cancer* **15** 475-
588 483.
- 589 Hershberger PA, Stabile LP, Kanterewicz B, Rothstein ME, Gubish CT, Land S, Shuai Y,
590 Siegfried JM & Nichols M 2009 Estrogen receptor beta (ERbeta) subtype-specific ligands
591 increase transcription, p44/p42 mitogen activated protein kinase (MAPK) activation
592 and growth in human non-small cell lung cancer cells. *J Steroid Biochem Mol Biol* **116**
593 102-109.
- 594 Jala VR, Radde BN, Haribabu B & Klinge CM 2012 Enhanced expression of G-protein
595 coupled estrogen receptor (GPER/GPR30) in lung cancer. *BMC Cancer* **12** 624.
- 596 Jemal A, Miller KD, Ma J, Siegel RL, Fedewa SA, Islami F, Devesa SS & Thun MJ 2018
597 Higher Lung Cancer Incidence in Young Women Than Young Men in the United States. *N*
598 *Engl J Med* **378** 1999-2009.
- 599 Johnson KE, Forward JA, Tippy MD, Ceglowski JR, El-Husayni S, Kulenthirarajan R,
600 Machlus KR, Mayer EL, Italiano JE, Jr. & Battinelli EM 2017 Tamoxifen Directly Inhibits
601 Platelet Angiogenic Potential and Platelet-Mediated Metastasis. *Arterioscler Thromb Vasc*
602 *Biol* **37** 664-674.
- 603 Katcoff H, Wenzlaff AS & Schwartz AG 2014 Survival in women with NSCLC: the role of
604 reproductive history and hormone use. *J Thorac Oncol* **9** 355-361.
- 605 Kim KH, Young BD & Bender JR 2014 Endothelial estrogen receptor isoforms and
606 cardiovascular disease. *Mol Cell Endocrinol* **389** 65-70.

- 607 Kisanuki YY, Hammer RE, Miyazaki J, Williams SC, Richardson JA & Yanagisawa M 2001
608 Tie2-Cre transgenic mice: a new model for endothelial cell-lineage analysis in vivo. *Dev*
609 *Biol* **230** 230-242.
- 610 Lewis DR, Check DP, Caporaso NE, Travis WD & Devesa SS 2014 US lung cancer trends
611 by histologic type. *Cancer* **120** 2883-2892.
- 612 Liu C, Liao Y, Fan S, Tang H, Jiang Z, Zhou B, Xiong J, Zhou S, Zou M & Wang J 2015 G
613 protein-coupled estrogen receptor (GPER) mediates NSCLC progression induced by
614 17beta-estradiol (E2) and selective agonist G1. *Med Oncol* **32** 104.
- 615 Mah V, Seligson DB, Li A, Marquez DC, Wistuba, II, Elshimali Y, Fishbein MC, Chia D,
616 Pietras RJ & Goodglick L 2007 Aromatase expression predicts survival in women with
617 early-stage non small cell lung cancer. *Cancer Res* **67** 10484-10490.
- 618 Mahmoodzadeh S, Leber J, Zhang X, Jaisser F, Messaoudi S, Morano I, Furth PA,
619 Dworatzek E & Regitz-Zagrosek V 2014 Cardiomyocyte-specific Estrogen Receptor
620 Alpha Increases Angiogenesis, Lymphangiogenesis and Reduces Fibrosis in the Female
621 Mouse Heart Post-Myocardial Infarction. *J Cell Sci Ther* **5** 153.
- 622 Morfoisse F, Tatin F, Chaput B, Therville N, Vaysse C, Metivier R, Malloizel-Delaunay J,
623 Pujol F, Godet AC, De Toni F, et al. 2018 Lymphatic Vasculature Requires Estrogen
624 Receptor-alpha Signaling to Protect From Lymphedema. *Arterioscler Thromb Vasc Biol*
625 **38** 1346-1357.
- 626 Nowak-Sliwinska P, Alitalo K, Allen E, Anisimov A, Aplin AC, Auerbach R, Augustin HG,
627 Bates DO, van Beijnum JR, Bender RHF, et al. 2018 Consensus guidelines for the use and
628 interpretation of angiogenesis assays. *Angiogenesis*.
- 629 Paupert J, Sounni NE & Noel A 2011 Lymphangiogenesis in post-natal tissue remodeling:
630 lymphatic endothelial cell connection with its environment. *Mol Aspects Med* **32** 146-
631 158.
- 632 Pequeux C, Raymond-Letron I, Blacher S, Boudou F, Adlanmerini M, Fouque MJ, Rochaix
633 P, Noel A, Foidart JM, Krust A, et al. 2012 Stromal estrogen receptor-alpha promotes
634 tumor growth by normalizing an increased angiogenesis. *Cancer Res* **72** 3010-3019.
- 635 Petrova TV & Koh GY 2018 Organ-specific lymphatic vasculature: From development to
636 pathophysiology. *J Exp Med* **215** 35-49.
- 637 Pietras RJ, Marquez DC, Chen HW, Tsai E, Weinberg O & Fishbein M 2005 Estrogen and
638 growth factor receptor interactions in human breast and non-small cell lung cancer cells.
639 *Steroids* **70** 372-381.
- 640 Pietras RJ & Marquez-Garban DC 2007 Membrane-associated estrogen receptor
641 signaling pathways in human cancers. *Clin Cancer Res* **13** 4672-4676.
- 642 Raso MG, Behrens C, Herynk MH, Liu S, Prudkin L, Ozburn NC, Woods DM, Tang X,
643 Mehran RJ, Moran C, et al. 2009 Immunohistochemical expression of estrogen and
644 progesterone receptors identifies a subset of NSCLCs and correlates with EGFR
645 mutation. *Clin Cancer Res* **15** 5359-5368.
- 646 Rocks N, Bekaert S, Coia I, Paulissen G, Gueders M, Evrard B, Van Heugen JC, Chiap P,
647 Foidart JM, Noel A, et al. 2012 Curcumin-cyclodextrin complexes potentiate gemcitabine
648 effects in an orthotopic mouse model of lung cancer. *Br J Cancer* **107** 1083-1092.

- 649 Rodriguez-Lara V, Hernandez-Martinez JM & Arrieta O 2018 Influence of estrogen in
650 non-small cell lung cancer and its clinical implications. *J Thorac Dis* **10** 482-497.
- 651 Rouquette I, Lauwers-Cances V, Allera C, Brouchet L, Milia J, Nicaise Y, Laurent J, Delisle
652 MB, Favre G, Didier A, et al. 2012 Characteristics of lung cancer in women: importance of
653 hormonal and growth factors. *Lung Cancer* **76** 280-285.
- 654 Schabath MB, Wu X, Vassilopoulou-Sellin R, Vaporciyan AA & Spitz MR 2004 Hormone
655 replacement therapy and lung cancer risk: a case-control analysis. *Clin Cancer Res* **10**
656 113-123.
- 657 Schleidgen S, Klingler C, Bertram T, Rogowski WH & Marckmann G 2013 What is
658 personalized medicine: sharpening a vague term based on a systematic literature
659 review. *BMC Med Ethics* **14** 55.
- 660 Siegfried JM 2001 Women and lung cancer: does oestrogen play a role? *Lancet Oncol* **2**
661 506-513.
- 662 Siegfried JM & Stabile LP 2014 Estrogenic steroid hormones in lung cancer. *Semin*
663 *Oncol* **41** 5-16.
- 664 Stabile LP, Davis AL, Gubish CT, Hopkins TM, Luketich JD, Christie N, Finkelstein S &
665 Siegfried JM 2002 Human non-small cell lung tumors and cells derived from normal lung
666 express both estrogen receptor alpha and beta and show biological responses to
667 estrogen. *Cancer Res* **62** 2141-2150.
- 668 Stanhewicz AE, Wenner MM & Stachenfeld NS 2018 Sex differences in endothelial
669 function important to vascular health and overall cardiovascular disease risk across the
670 lifespan. *Am J Physiol Heart Circ Physiol*.
- 671 Suzuma I, Mandai M, Takagi H, Suzuma K, Otani A, Oh H, Kobayashi K & Honda Y 1999 17
672 Beta-estradiol increases VEGF receptor-2 and promotes DNA synthesis in retinal
673 microvascular endothelial cells. *Invest Ophthalmol Vis Sci* **40** 2122-2129.
- 674 Tang H, Liao Y, Zhang C, Chen G, Xu L, Liu Z, Fu S, Yu L & Zhou S 2014 Fulvestrant-
675 mediated inhibition of estrogen receptor signaling slows lung cancer progression. *Oncol*
676 *Res* **22** 13-20.
- 677 Townsend EA, Miller VM & Prakash YS 2012 Sex differences and sex steroids in lung
678 health and disease. *Endocr Rev* **33** 1-47.
- 679 Wakelee HA, Chang ET, Gomez SL, Keegan TH, Feskanich D, Clarke CA, Holmberg L, Yong
680 LC, Kolonel LN, Gould MK, et al. 2007 Lung cancer incidence in never smokers. *J Clin*
681 *Oncol* **25** 472-478.
- 682 Wakelee HA, Wang W, Schiller JH, Langer CJ, Sandler AB, Belani CP, Johnson DH &
683 Eastern Cooperative Oncology G 2006 Survival differences by sex for patients with
684 advanced non-small cell lung cancer on Eastern Cooperative Oncology Group trial 1594.
685 *J Thorac Oncol* **1** 441-446.
- 686 Wong BW, Zecchin A, Garcia-Caballero M & Carmeliet P 2018 Emerging Concepts in
687 Organ-Specific Lymphatic Vessels and Metabolic Regulation of Lymphatic Development.
688 *Dev Cell* **45** 289-301.
- 689 Zhan P, Wang J, Lv XJ, Wang Q, Qiu LX, Lin XQ, Yu LK & Song Y 2009 Prognostic value of
690 vascular endothelial growth factor expression in patients with lung cancer: a systematic
691 review with meta-analysis. *J Thorac Oncol* **4** 1094-1103.

692 Zhang L, Zhou F, Han W, Shen B, Luo J, Shibuya M & He Y 2010 VEGFR-3 ligand-binding
693 and kinase activity are required for lymphangiogenesis but not for angiogenesis. *Cell Res*
694 **20** 1319-1331.

695 Zhao G, Zhao S, Wang T, Zhang S, Lu K, Yu L & Hou Y 2011 Estrogen receptor beta
696 signaling regulates the progression of Chinese non-small cell lung cancer. *J Steroid*
697 *Biochem Mol Biol* **124** 47-57.

698

699

1 **Figure Legends**

2 **Figure 1. Orthotopic graft of LLC-Luc cells into lung parenchyma grows faster in**
3 **females than in males.** (A) *In vivo* bioluminescent signals derived from LLC-Luc lung
4 tumours imaged either in whole mice (upper panel) or in dissected pulmonary lobes (lower
5 panel) from male and female mice. The right panel shows bioluminescent intensity
6 quantification over time (n=8), **p<0.01, 2-way ANOVA. (B) Hematoxylin/Eosin staining of
7 LLC-Luc lung tumours from male (n=24) and female (n=23) mice (scale bar=1mm) and
8 quantification of lung tumour density (tumour area/total lung area) on the right panel, 8 slides
9 spaced with 50µm were analysed per sample, *p<0.05, Mann-Whitney. (C) *In vivo*
10 bioluminescent signals derived from LLC-Luc lung tumours imaged either in whole mice of
11 female, OVX female and OVX+E2 female mice. The right panel shows bioluminescent
12 intensity quantification over time (n=8), *p<0.05, 2-way ANOVA. (D) Hematoxylin/Eosin
13 staining and quantification of lung tumour density (tumour area/total lung area) of LLC-Luc
14 lung tumours from females and OVX female mice treated or not with E2 (scale bar=1mm)
15 (n=8), 8 slides spaced with 50µm were analysed per sample, *p<0.05, 1-way ANOVA. (E) *In*
16 *vivo* bioluminescent signals derived from LLC-Luc lung tumours imaged either in whole mice
17 of male (n=8), gonadectomized (Cx) male (n=8) and Cx+E2 male (n=7) animals. The right
18 panel shows bioluminescent intensity quantification over time, 2-way ANOVA. (F)
19 Hematoxylin/Eosin staining and quantification of the lung tumour density (tumour area/total
20 lung area) of LLC-Luc lung tumours from males (n=8) and gonadectomized male mice
21 treated (Cx+E2, n=7) or not with E2 (Cx, n=8) (scale bar=1mm), 8 slides spaced with 50µm
22 were analysed per sample, 1-way ANOVA.

23

24 **Figure 2. E2 increases LLC-Luc cell proliferation *in vivo*, but not *in vitro*.** (A) Western
25 Blot of estrogen receptors (ER) on LLC-Luc cell lysates: ERa (66kDa), ERb (56kDa), GPER

26 (42kDa). HSC70 (70kDa) was used as loading control. Proteins isolated from mouse ovary
27 and testis were used as positive controls. (B) *In vitro* proliferation of LLC-Luc cells treated
28 with vehicle, E2 (10^{-9} M) or FBS 10% (positive control) for 24, 48 and 72h, *** $p < 0.001$ vs
29 vehicle, $n=6$, 2-way ANOVA. (C) *In vitro* proliferation of LLC-Luc cells treated with vehicle,
30 E2 (10^{-10} M to 10^{-7} M) or FBS 10% (positive control) for 48h, *** $p < 0.001$ vs vehicle, $n=6$, 1-
31 way ANOVA. (D) *In vitro* viability of LLC-Luc cells treated with vehicle, E2 (10^{-10} M to 10^{-7} M)
32 or cisplatin (10^{-4} M, positive control) for 48h, *** $p < 0.001$ vs vehicle, $n=6$, 1-way
33 ANOVA. (E) *In vitro* proliferation of LLC-Luc cells treated with ERa, ERb or GPER
34 selective antagonists (MPP 10^{-8} M, PHTPP 10^{-8} M, G15 10^{-7} M) in combination or not with E2
35 (10^{-9} M), $n=6$, 1-way ANOVA. (F) *In vivo* LLC-Luc cell proliferation analysed by EdU
36 immunofluorescent staining (scale bar= $500\mu\text{m}$ in upper panel, scale bar= $100\mu\text{m}$ in lower
37 panel) in OVX female mice treated or not with E2. (G) Quantification of EdU density (EdU
38 area/lung tumour area) on LLC-Luc tumours from OVX-females ($n=26$) and OVX+E2
39 females ($n=23$), * $p < 0.05$, t-test. (H) Double-immunofluorescent staining and their zoom of
40 LYVE1 (red) and ERa (green), colocalisation of stainings (yellow) and DAPI (blue) in LLC-
41 Luc lung tumours, scale bar= $50\mu\text{m}$. Uterus tissue was used as positive control, scale
42 bar= $50\mu\text{m}$. (I) Double-immunofluorescent staining and their zoom of CD31 (red) and ERa
43 (green), colocalisation of stainings (yellow) and DAPI (blue) in LLC-Luc lung tumours, scale
44 bar= $50\mu\text{m}$.

45

46 **Figure 3. E2 increases lymph/angiogenesis through ERa.** (A) Immunofluorescent staining
47 (scale bar= $50\mu\text{m}$) of LYVE1 (green) or CD31 (red) in LLC-Luc lung tumours from female
48 ($n=11$), OVX ($n=15$) or OVX+E2-treated ($n=18$) female mice, and from male ($n=12$), Cx
49 ($n=5$) or Cx+E2-treated ($n=5$) male mice. (B) Quantification of LYVE1 density (LYVE1
50 area/lung tumour area) and CD31 density (CD31 area/lung tumour area) in lung tumours of

51 these mice, * $p < 0.05$; ** $p < 0.01$, Mann-Whitney or 1-way ANOVA. (C) VEGFC, (D)
52 VEGFD, (E) VEGFA and (F) bFGF levels measured by Milliplex and reported to the total
53 amount of protein (mg) in lung tumour lysates issued from male, female, OVX-female and
54 OVX+E2 female mice, * $p < 0.05$, 1-way ANOVA. (G) CD31/LYVE1 staining (for each
55 condition: left panel, scale bar=1mm; right panel, scale bar=500 μ m) and quantification
56 (CD31 or LYVE1 area/total cornea area) in cornea of female mice (n=10), OVX (n=10) or
57 OVX+E2 (n=10) mice, * $p < 0.05$; *** $p < 0.001$, 1-way ANOVA, or (H) in cornea of male
58 (n=18) or castrated male mice (Cx, n=8), Mann-Whitney.

59

60 **Figure 4. Prolymphangiogenic and proangiogenic effects of E2 are mediated by ER α .** (A)

61 Hematoxylin/Eosin (H/E) staining of LLC-Luc lung tumours issued from Tie2-Cre⁻/ER α ^{lox/lox}
62 male (n=7) or female (n=7) mice and from Tie2-Cre⁺/ER α ^{lox/lox} male (n=8) or female (n=5)
63 mice (scale bar=1mm) and quantification of the tumour density (tumour area/total lung area),
64 8 slides spaced by 50 μ m were analysed per sample, * $p < 0.05$, Mann-Whitney. (B)
65 Hematoxylin/Eosin (H/E) staining of LLC-Luc lung tumours from Tie2-Cre⁻/ER α ^{lox/lox} OVX
66 (n=6), OVX+E2 (n=6) female mice and from Tie2-Cre⁺/ER α ^{lox/lox} OVX (n=7), OVX+E2
67 (n=5) female mice (scale bar=1mm) and quantification of the tumour density (tumour
68 area/total lung area), 8 slides spaced by 50 μ m were analysed per sample, * $p < 0.05$, Mann-
69 Whitney. (C) LYVE1 immunofluorescent staining (scale bar=50 μ m) and quantification
70 (LYVE1 area/lung tumour area) in LLC-Luc lung tumours in Tie2-Cre⁺/ER α ^{lox/lox} male (n=8),
71 female (n=5), female OVX (n=7) and female OVX+E2 (n=5) mice, Kruskal-Wallis. (D)
72 CD31 immunofluorescent staining (scale bar=50 μ m) and quantification (CD31 area/lung
73 tumour area) in LLC-Luc lung tumours in Tie2-Cre⁺/ER α ^{lox/lox} male (n=8), female (n=5),
74 female OVX (n=7) and female OVX+E2 (n=5) Kruskal-Wallis. (E) LYVE1/CD31 staining
75 (scale bar=500 μ m) and quantification (LYVE1 or CD31 area/total cornea area) of blood and

76 lymphatic vessels in cornea of Tie2-Cre⁺/ERa^{lox/lox} male (n=8), female (n=5), OVX female
77 (n=7) and OVX+E2 female (n=5) mice, Kruskal-Wallis. (F) LYVE1/CD31 staining (scale
78 bar=500µm) and quantification (LYVE1 or CD31 area/total cornea area) of blood and
79 lymphatic vessels in cornea of wild-type female mice treated with vehicle (n=11), ERa
80 antagonist (MPP 10⁻⁸M, n=13), ERb antagonist (PHTPP 10⁻⁸M, n=12) or GPER antagonist
81 (G15 10⁻⁷M, n=9), *p<0.05, Kruskal-Wallis.

82

83 **Figure 5. Lung tumour treatment with ERa or ERb antagonist or with tamoxifen.** (A) *In*
84 *vivo* bioluminescent signals and quantification of LLC-Luc lung tumours in female mice
85 treated with vehicle (control group), ERa antagonist (MPP, 1mg/kg), ERb antagonist (PHTPP,
86 1mg/kg), n=8; *p<0.05, 2-way ANOVA. (B) Hematoxylin/Eosin staining of LLC-Luc lung
87 tumours (scale bar=1mm) and quantification of tumour density (lung tumour area/total lung
88 area) in females treated with vehicle; MPP; PHTPP and Tamoxifen (Tmx), *p<0.05, Mann-
89 Whitney. (C) Immunofluorescent staining of CD31 positive blood vessels in LLC-Luc lung
90 tumours (scale bar=50µm) and quantification of the CD31 density (CD31 area/lung tumour
91 area) in tumours of female mice treated with vehicle (n=16), MPP (n=8); PHTPP (n=8) or
92 Tmx (n=8), **p<0.01, ***p<0.001, Kruskal-Wallis. (D) Immunofluorescent staining (scale
93 bar=50µm) and quantification (LYVE1 area/lung tumour area) of LYVE1 positive vessels in
94 LLC-Luc lung tumours of female mice treated with vehicle (n=7), MPP (n=8); PHTPP (n=7)
95 or Tmx (n=8), *p<0.05, **p<0.01, 1-way ANOVA. Milliplex analysis of (E) VEGFC, (F)
96 VEGFD, (G) VEGFA, (H) bFGF concentrations in LLC-Luc lung tumour lysates from
97 vehicle-, MPP- and Tmx-treated females; *p<0.05, **p<0.01, 1-way ANOVA. (I) *In vivo*
98 bioluminescent signals and quantification of LLC-Luc-derived bioluminescence in lungs of
99 male mice treated with vehicle (control group), ERa antagonist (MPP, 1mg/kg), ERb
100 antagonist (PHTPP, 1mg/kg) (n=8), 2-way ANOVA. (J) Hematoxylin/Eosin staining of LLC-

101 Luc lung tumours (scale bar=1mm) and quantification of tumour density (lung tumour
102 area/total lung area) from males treated with vehicle, MPP, PHTPP and Tamoxifen (Tmx),
103 Kruskal-Wallis. (K) Immunofluorescent staining of CD31 positive blood vessels in LLC-Luc
104 lung tumours (scale bar=50 μ m) and quantification of the CD31 density (CD31 area/lung
105 tumour area) in lung tumours of male mice (n=17), treated with vehicle (n=8), MPP (n=7);
106 PHTPP (n=7) or Tmx (n=7), Kruskal-Wallis. (L) Immunofluorescent staining (scale
107 bar=50 μ m) and quantification (LYVE1 area/lung tumour area) of LYVE1 positive vessels in
108 LLC-Luc lung tumours of male mice, treated with vehicle (n=8), MPP (n=6); PHTPP (n=7) or
109 Tmx (n=7), 1-way ANOVA.

110

111 **Figure 6. Lymph/angiogenic vasculature and ER α status in human lung**
112 **adenocarcinoma biopsies.** (A) Characteristics of human lung tumours (histology, age,
113 smoker status). (B) Representative immunohistochemical staining of ER α (blue) in human
114 lung tumour biopsies according to sex (men: n=23, women: n=51) and separated as ER α -
115 positive (ER α +) and ER α -negative (ER-) tumours, scale bar=50 μ m. (C) Immunofluorescent
116 staining of PDPN and quantification of PDPN density (PDPN stained tumour area/lung
117 tumour area) in human lung tumours according to sex (men n=23, women n=49) and ER α
118 expression (ER α + : men=14, women n=30; ER α - : men n=9, women n=19), *p<0.05;
119 **p<0.01; ***p<0.001, Mann-Whitney, scale bar=250 μ m on upper panel and 50 μ m on lower
120 panel. (D) Immunohistochemical staining of CD31 and quantification (CD31 stained tumour
121 area/lung tumour area) in human lung tumours according to sex (men n=23, women n=51)
122 and ER α expression (ER α + : men=14, women n=30; ER α - : men n=9, women n=19), *p<0.05,
123 t-test, scale bar=250 μ m on upper panel and 50 μ m on lower panel. (E) Representative ER α
124 (green), PDPN (red) and CD31 (red) mRNA detection by RNAscope on human lung tumour

125 sections (scale bar=10 μ m). Endometrium is used as positive control for ER α expression. Cell
126 nuclei are stained with DAPI.

127

128 **Supplementary figure legends**

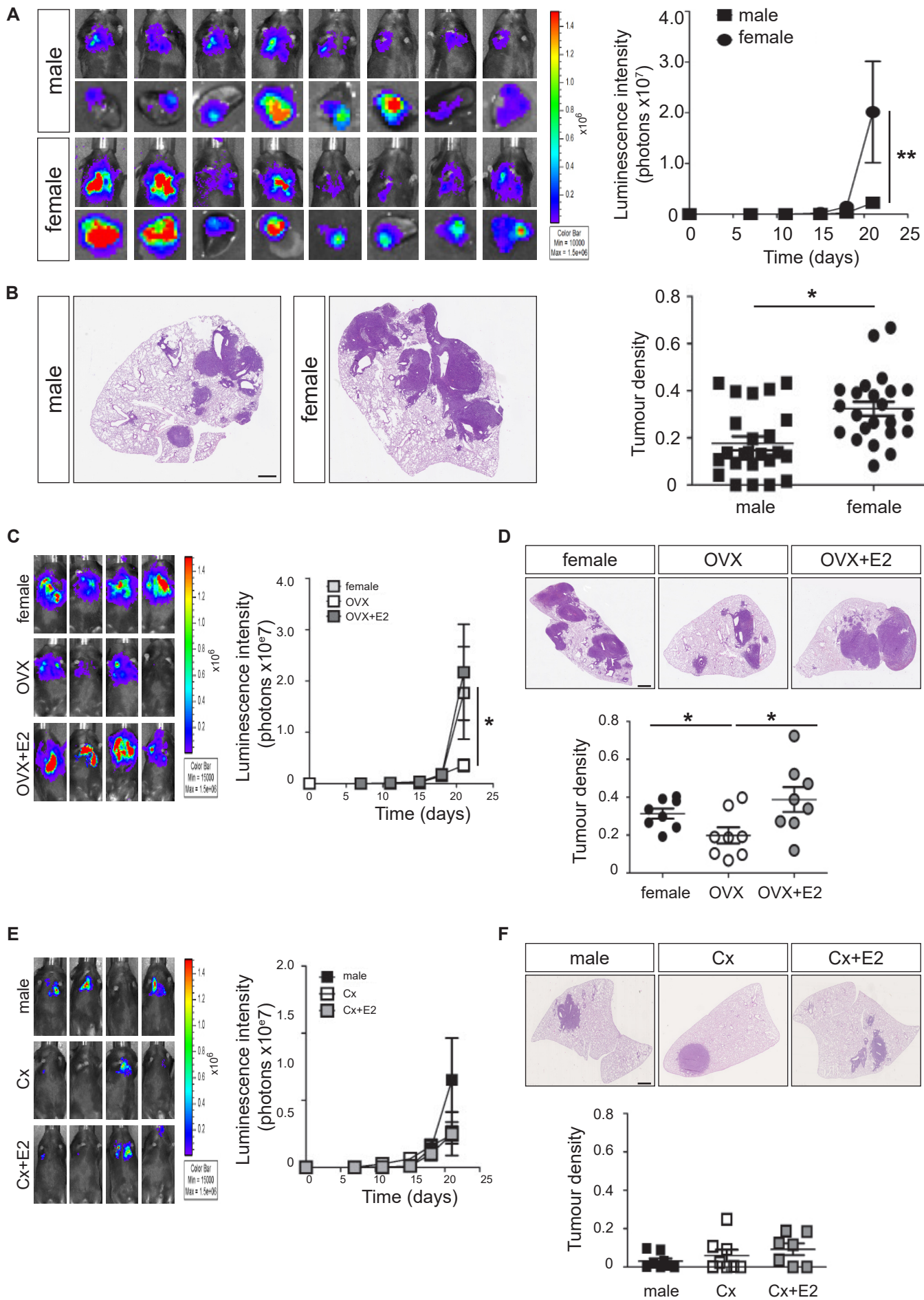
129

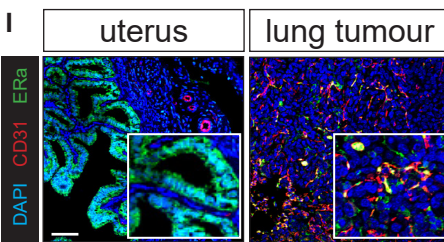
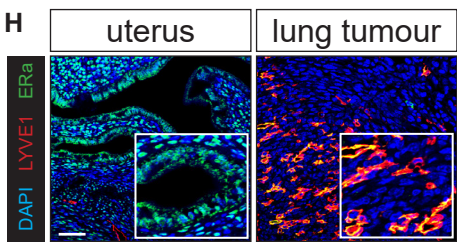
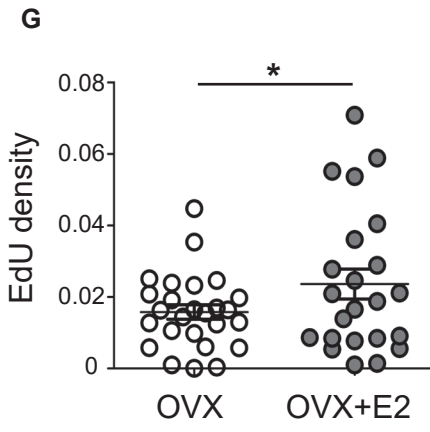
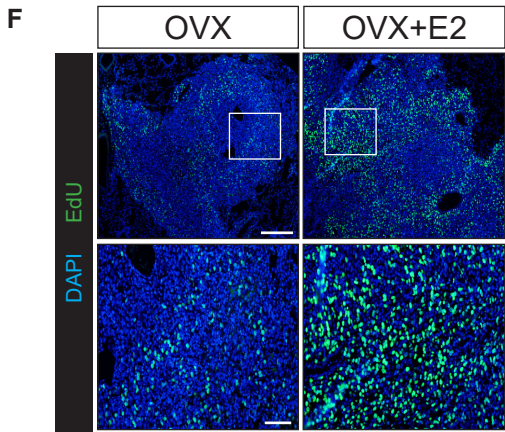
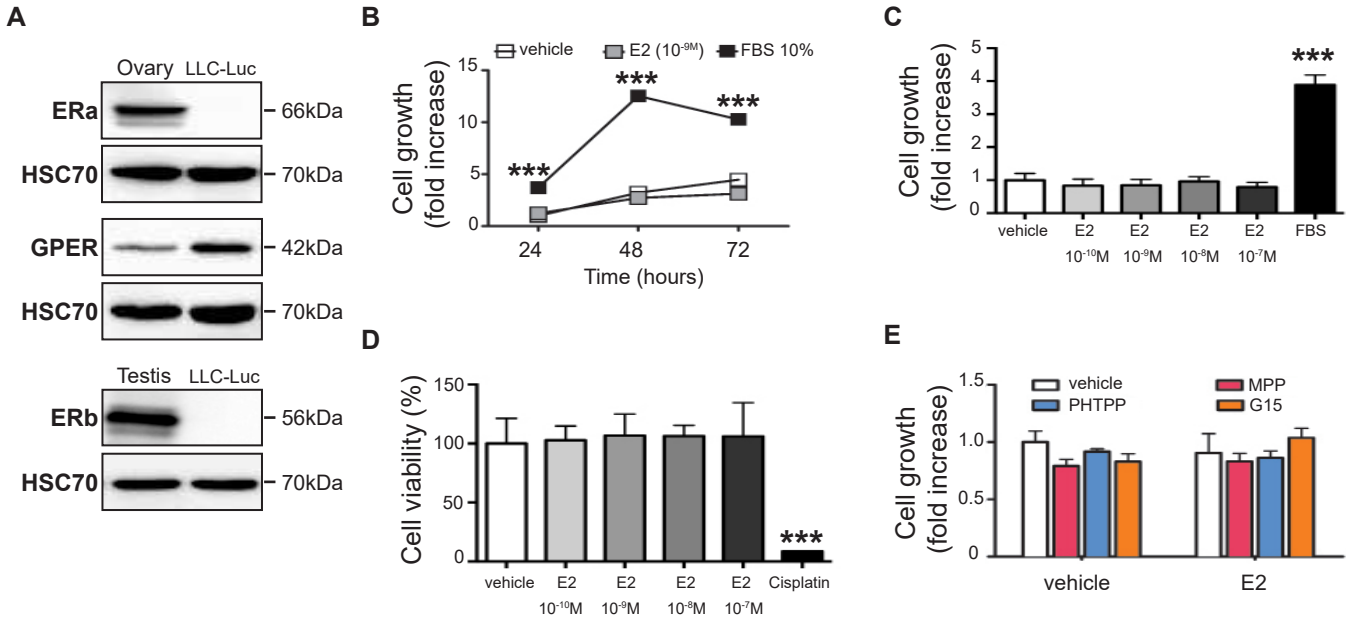
130 **Suppl. Fig.1:** Genotyping of Tie2-Cre⁺/ER α ^{lox/lox} (Cre+) and Tie2-Cre⁻/ER α ^{lox/lox} (Cre-) mice
131 by PCR on DNA extracts from the tail. A. Expression of Cre-recombinase and of FGF2 used
132 as internal positive control of PCR. B. Expression of ER α ^{lox/lox} and of ER α ^{-/-} corresponding to
133 *esr1* without exon 2.

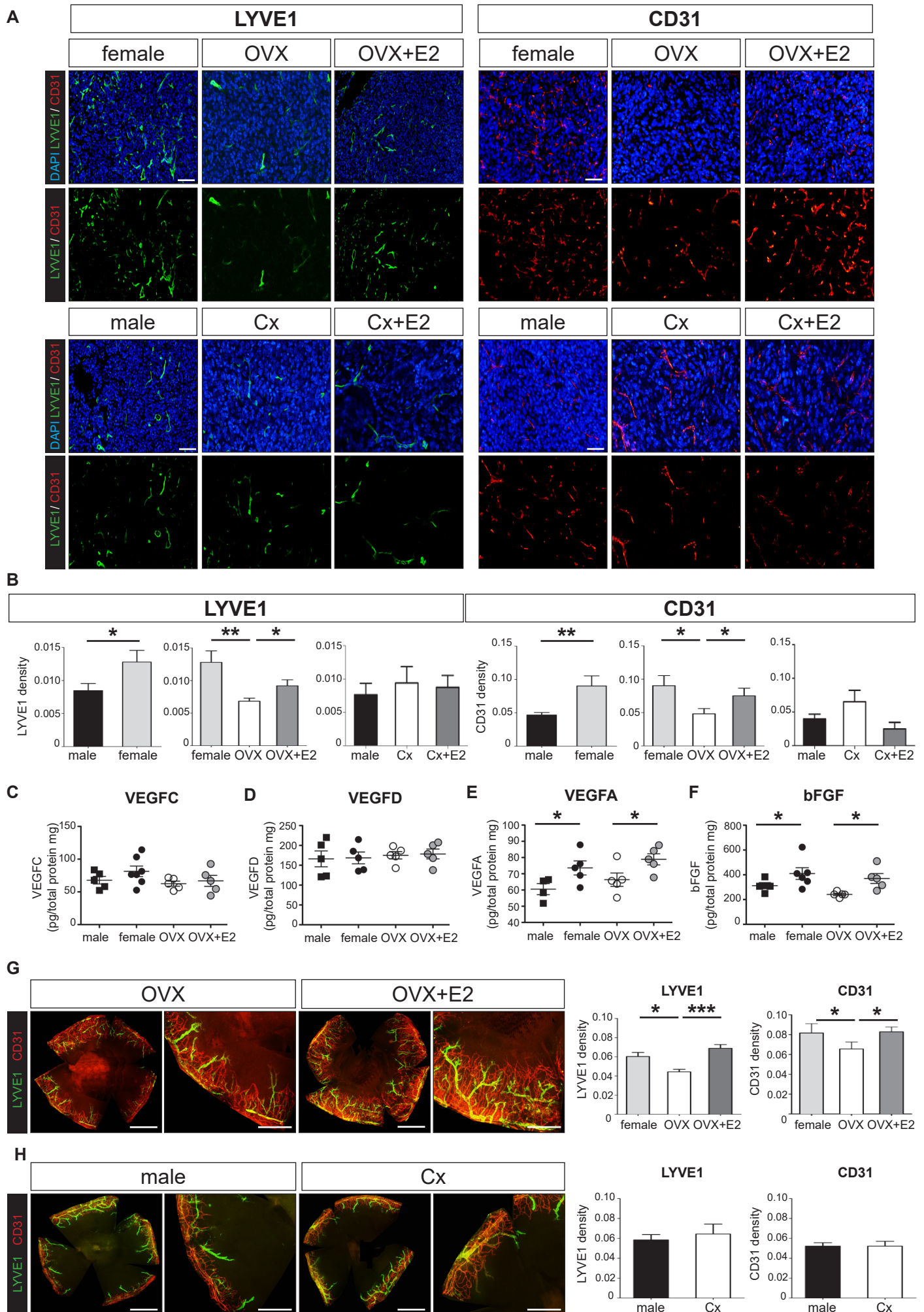
134

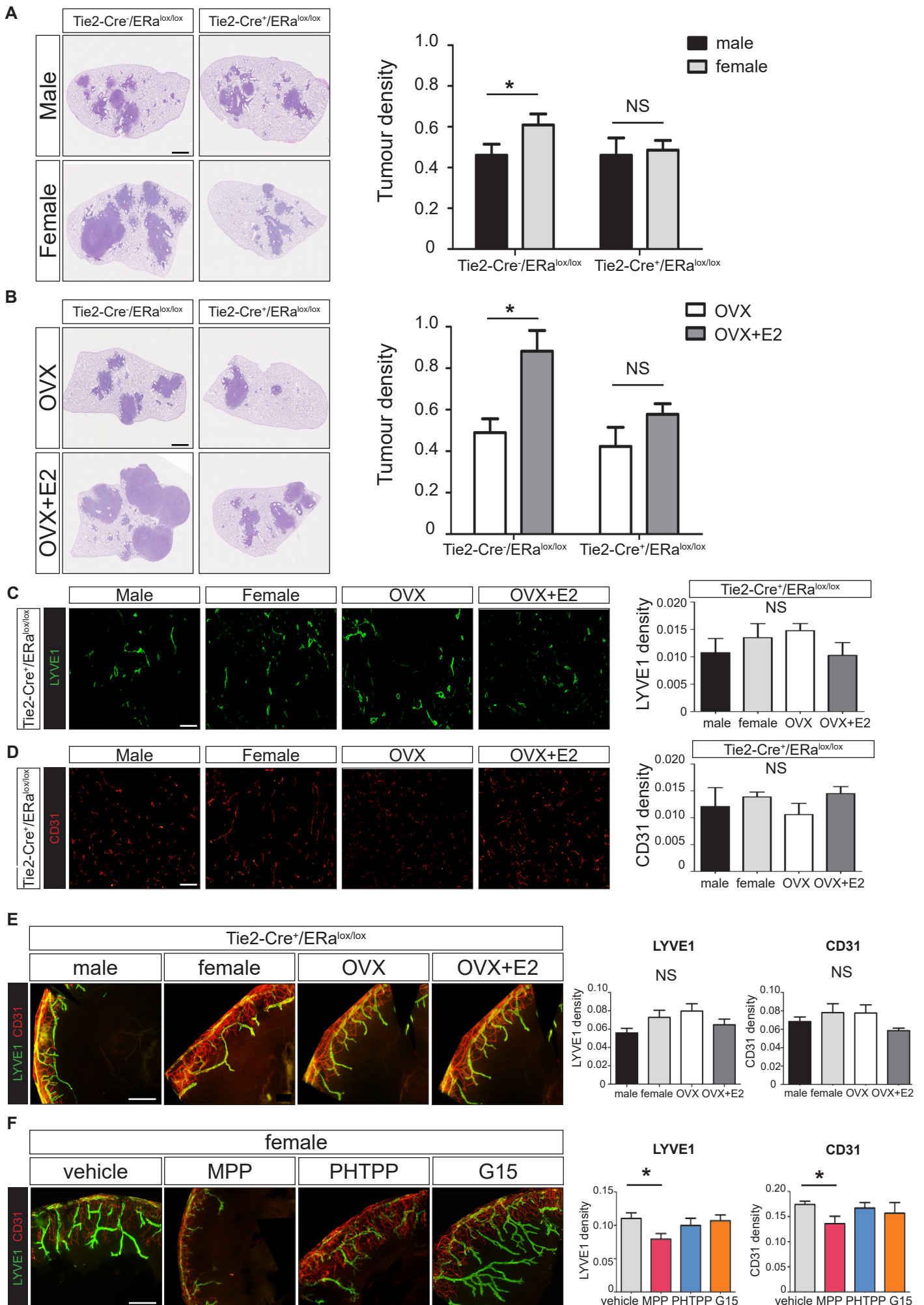
135 **Suppl. Fig.2:** ELISA quantification of (A) VEGFA and (B) bFGF in LLC-Luc lung tumour
136 lysates from vehicle- and PHTPP-treated females.

137



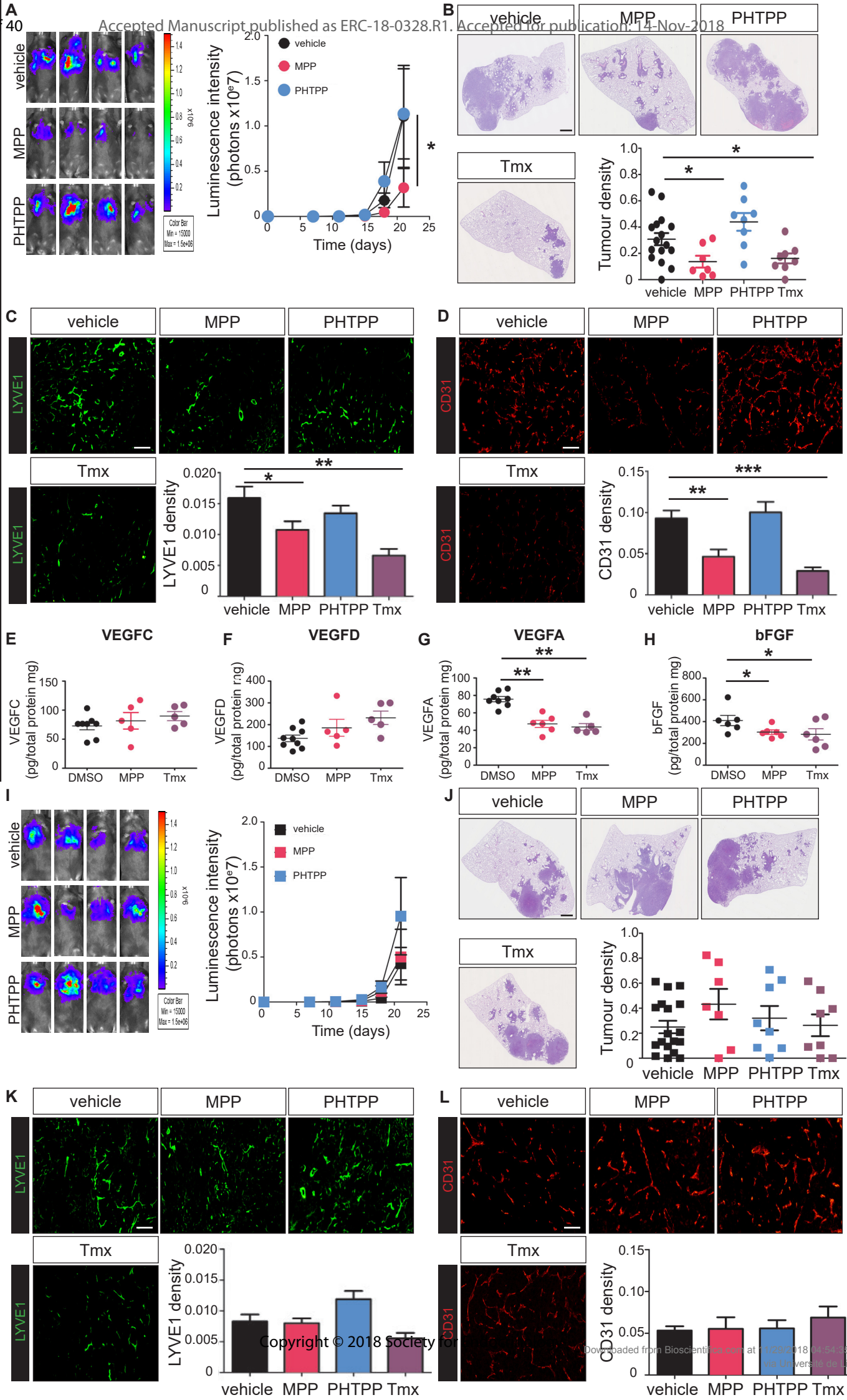


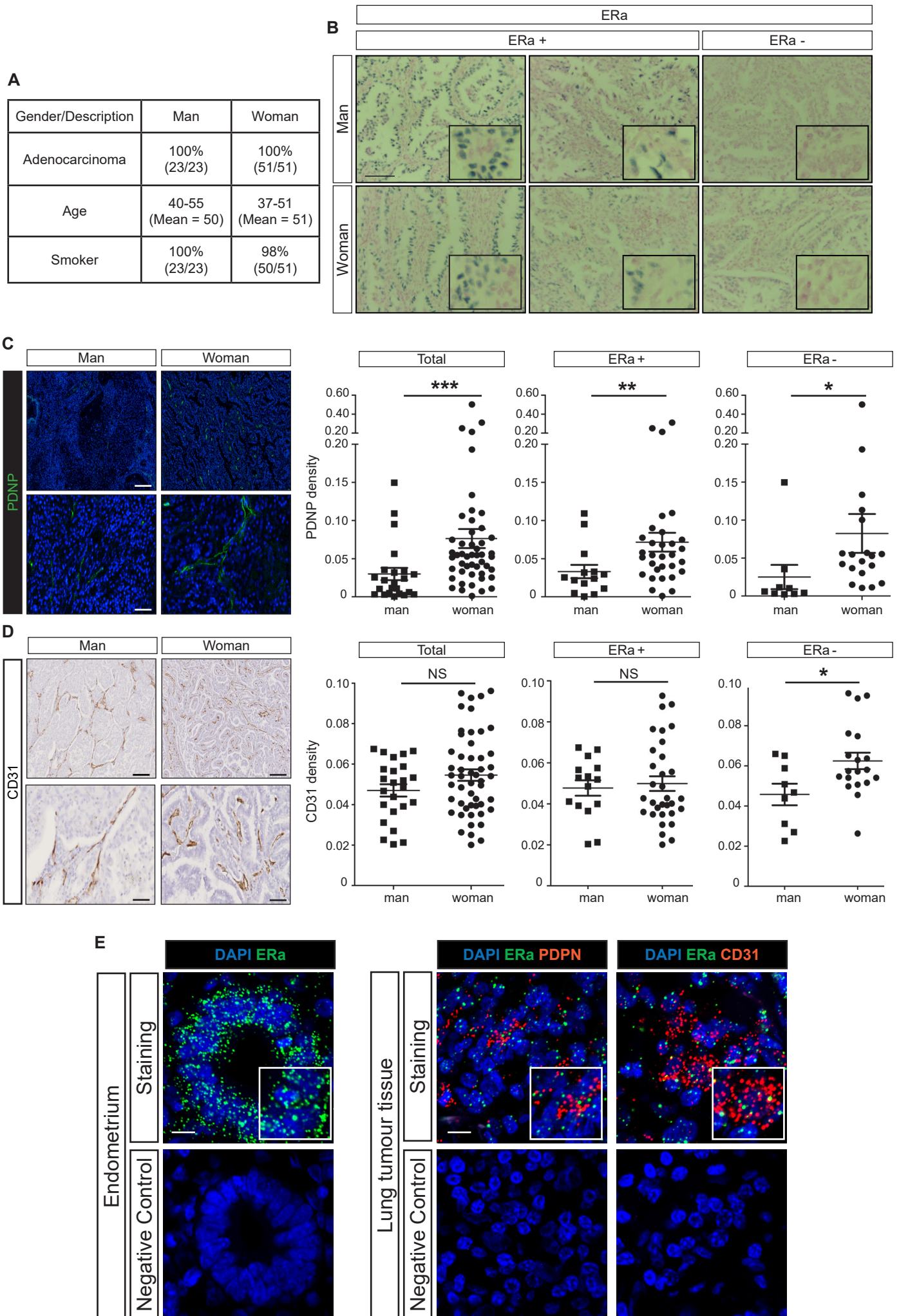


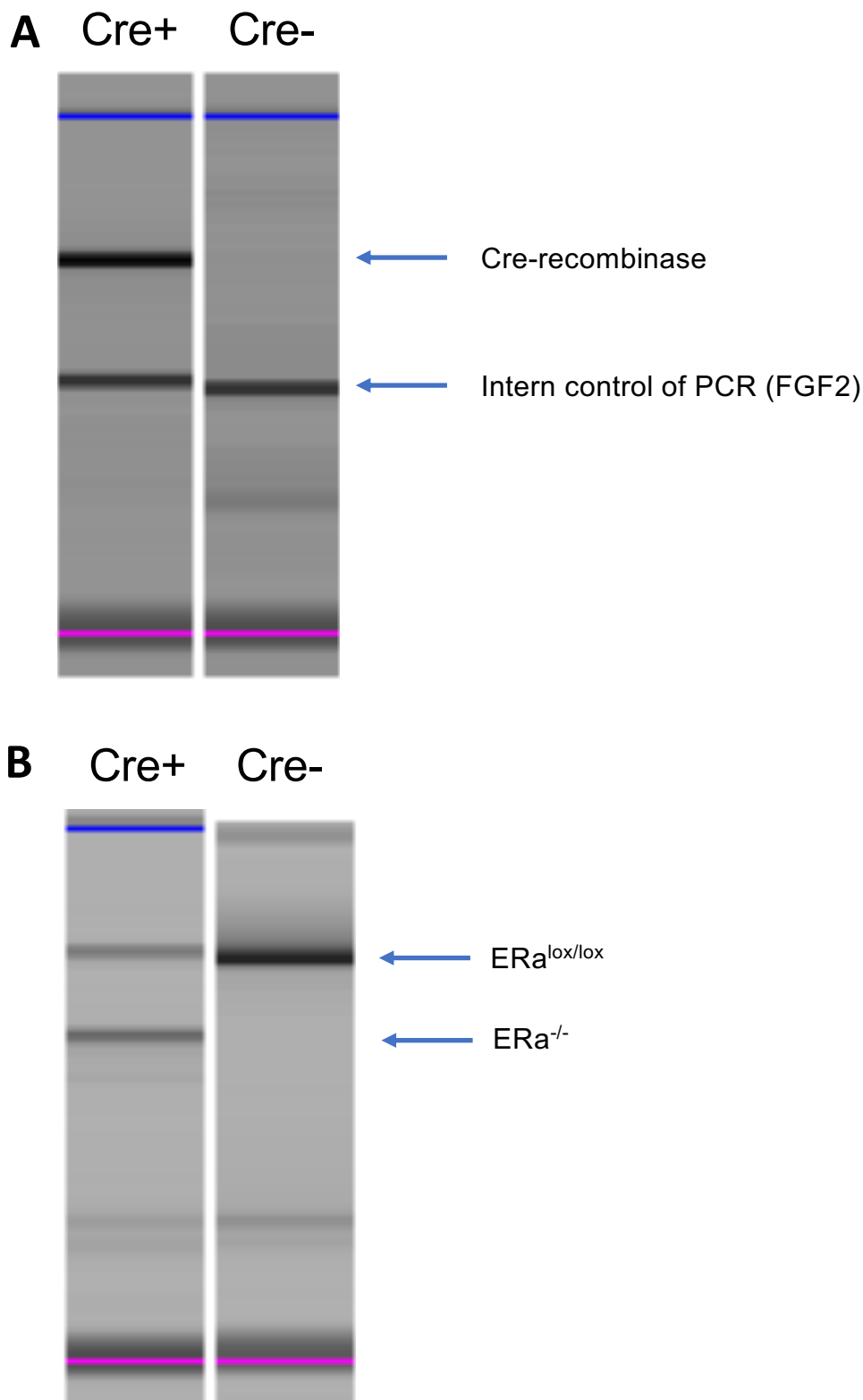


FEMALE

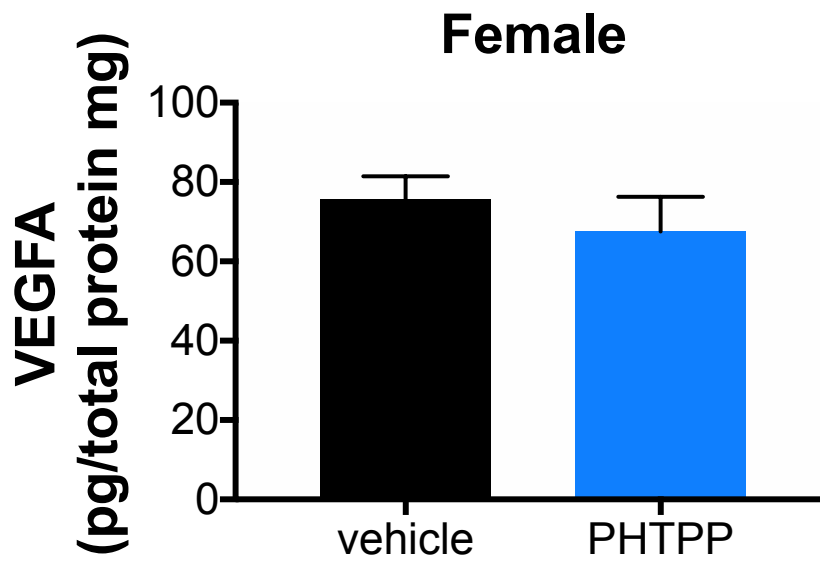
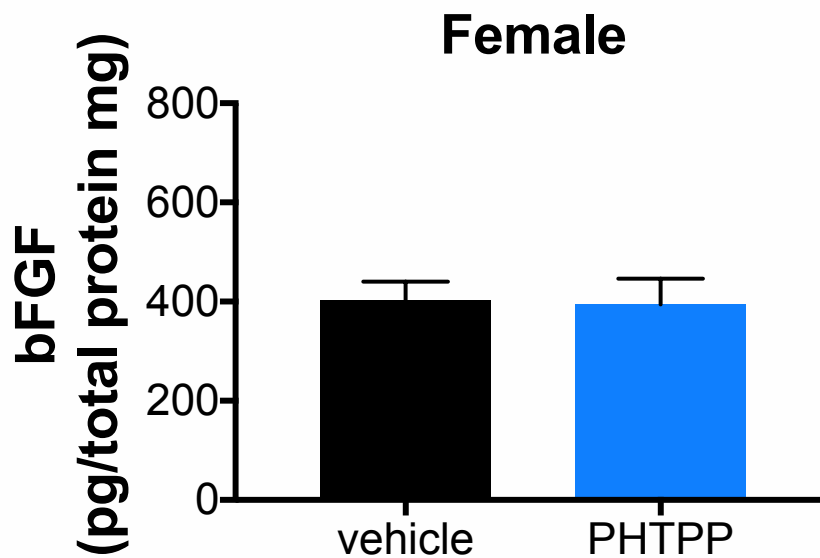
MALE







Suppl. Fig.1: Genotyping of Tie2-Cre⁺/ERa^{lox/lox} (Cre+) and Tie2-Cre⁻/ERa^{lox/lox} (Cre-) mice by PCR on DNA extracts from the tail. A. Expression of Cre-recombinase and of FGF2 used as internal positive control of PCR. B. Expression of ERa^{lox/lox} and of ERa^{-/-} corresponding to *esr1* without exon 2.

A**B**

Suppl. Fig.2: ELISA quantification of (A) VEGFA and (B) bFGF in LLC-Luc lung tumour lysates from vehicle- and PHTPP-treated females.